Injury, Int. J. Care Injured 48S5 (2017) S41–S46

Contents lists available at ScienceDirect

Injury

journal homepage: www.elsevier.com/locate/Injury

A biomechanical comparison of four fixed-angle dorsal plates in a finite element model of dorsally-unstable radius fracture

Josip Knežević[a,*], Janoš Kodvanj[b], Fabijan Čukelj[a], Frane Pamuković[b], Arsen Pavić[a]

[a]University Hospital Split, Department of Orthopaedic Trauma, Spinčićeva 1, 21000 Split, Croatia
[b]Faculty of Mechanical Engineering and Naval Architecture, University of Zagreb, Ivana Lučića 5, 10000 Zagreb, Croatia

KEYWORDS

radius fractures
internal fracture fixation
humans
anatomic models
biomechanics
computer simulation

ABSTRACT

Purpose: To compare the finite element models of two different composite radius fracture patterns, reduced and stabilised with four different fixed-angle dorsal plates during axial, dorsal and volar loading conditions.
Methods: Eight different plastic models representing four AO/ASIF type 23-A3 distal radius fractures and four AO/ASIF 23-C2 distal radius fractures were obtained and fixed each with 1 of 4 methods: a standard dorsal non-anatomical fixed angle T-plate (3.5 mm Dorsal T-plate, Synthes), anatomical fixed-angle double plates (2.4 mm LCP Dorsal Distal Radius, Synthes), anatomical fixed angle T-plate (2.4 mm Acu-Loc Dorsal Plate, Acumed) or anatomical variable-angle dorsal T-plate (3.5 mm, Dorsal Plate, Zrinski). Composite radius with plate and screws were scanned with a 3D optical scanner and later processed in Abaqus Software to generate the finite element model. All models were axially loaded at 3 points (centrally, volarly and dorsally) with 50 N forces to avoid the appearance of plastic deformations of the models. Total displacements at the end of the bone and the stresses in the bones and plates were determined and compared.
Results: Maximal von Mises stress in bone for 3-part fracture models was very similar to that in 2-part fracture models. The biggest difference between models and the largest displacements were seen during volar loading. The stresses in all models were the highest above the fracture gap. The best performance in all parameters tested was with the Zrinski plate and the most modest results were with the Synthes T-plate.
Conclusion: There was no significant difference between 2-part (AO/ASIF type 23-A3) and 3-part (AO/ASIF 23-C2) fracture models. Maximal stresses in the plates appeared above the fracture gap; therefore, it is worth considering the development of plates without screw holes above the gap.

Introduction

Distal radius fractures are among the most common skeletal injuries, accounting for 14% of all fractures [1,2]. The principles of treatment for distal radius fractures are anatomical reduction, stable fixation and early motion. The ways to achieve these goals include external fixation and open reduction and internal fixation.

In younger patients, ORIF is associated with a well-developed and firm cortex, and dense cancellous bone allows less strain on the screw-bone connection, thereby ensuring a stable stronghold for the screw and high pressure between the bone fragments, which reduces the possibility for osteolysis and development of microfracture on the contact surface [3]. In older patients with osteoporotic bones, stable osteosynthesis is possible only by increasing the contact surface between metallic implants and bone (which is not in accordance with the important preservation of local biological conditions, particularly the vitality of the bone), or by increasing the stability of the screw-plate connection. For this reason, we used fixed-angle volar plates to preserve vascularity and improve screw-plate stability [3,4].

Fixed-angle volar plates are favoured by many authors for dorsally-comminuted distal radius fractures because of fewer tendon complications and improved fixation [5–12].

When treating dorsally-unstable distal radius fractures, there is the theoretical concern about a disadvantage of volar plating in cantilever bending when the distal radius is axially loaded at a point dorsal to its neutral axis. This concern could lead to a delay in starting early postoperative rehabilitation.

Dorsal plating has some important indications, including excessive dorsal comminution, intra-articular reduction with direct articular visualisation and dorsal wedge osteotomy, when external forces may exceed the fixation capacity of a volar locking system. A large cohort

* Correspondence to: Department of Orthopaedic Trauma, Spinčićeva 1, 21000 Split, Croatia, Tel: +385 21 556 487; Fax: +385 21 556 587.
E-mail: knez64@gmail.com (J. Knežević).

0020-1383 / © 2017 Elsevier Ltd. All rights reserved.

study by Simic *et al*. found that extensor tendon irritation may not be as common in low-profile systems as in conventional systems [13–16]. They used low-profile systems and there were no cases of irritation, rupture or impedance of function of the extensor tendons. Furthermore, dorsal plates would be advantageous compared with volar plates because of their biomechanics (buttress effect) and ease-of-placement qualities [17–20].

If there is bone contact on the compression side, the bending strength of a plate placed on the tension side is about 100 times higher [21]. Thus, it is likely that the strength of the dorsal plate construct would be significantly increased by using it to fix the Colles' type fracture in which the volar cortical continuity was restored. Also, dorsally-applied plates may prevent redisplacement in some instances of dorsally-displaced metaphyseal fragments more reliably than volar plating [22].

Meanwhile, newer polyaxial dorsal-locking plates for distal radius allow insertion of a screw at a variable angle to meet the fracture pattern requirements to hold specific bone fragments.

Unfortunately, manufacturers usually do not reveal the actual stability of the polyaxial locking interfaces of their implants.

The aim of this study was to investigate the strength of three different dorsal radius polyaxial locking interfaces and to compare it with that of a standard dorsal locking T-plate using the finite element method.

Methods

In this study, the finite element analysis was performed to determine the stability of four locking plate constructs. The first construct was the standard dorsal non-anatomical plate (Synthes T) with monoaxial locking screws (3.5 mm Dorsal T-plate, Synthes). The second construct comprised an anatomical low-profile two dorsal plates system (Synthes DP) with monoaxial locking screws (2.4 mm LCP Dorsal Distal Radius, Synthes). The third construct was the low-profile anatomical dorsal plate with polyaxial locking screws (2.4 mm Acu-Loc Dorsal Plates, Acumed) and the forth construct was a new, low-profile anatomical dorsal plate with 15° tilting polyaxial locking screws (3.5 mm, Dorsal Plate, Zrinski).

The intact artificial right distal radius (SKU #1018–20, Sawbones Europe AB, Malmö, Sweden) was used in the present study.

The bone was wedged in its ends, the distal articular surface and the distal part of the radius body, which corresponds to real conditions for fixation of the radius at the elbow.

Two fracture models were made. Firstly, a 2-part osteotomy was created using an idealised planar cut: 1 cm transverse dorsal wedge osteotomy, centred 2 cm proximal to the articular surface of the lunate fossa with volar cortical contact, which simulates a 2-part extra-articular distal radius fracture with dorsal metaphyseal comminution (AO/ASIF 23-A3) (Figure 1a).

Secondly, a 3-part osteotomy was made like the first one, with the added sagittal split osteotomy between the scaphoid and lunate fossa creating an unstable intra-articular fracture with both radial styloid and ulnar-sided fracture fragment, which simulates a 3-part intra-articular distal radius fracture with dorsal metaphyseal comminution (AO/ASIF 23-C2) (Figure 1b).

The finite element models were generated based on 3D scans from an optical 3D scanner (Atos III Triple Scan, GOM mbH, Germany). The geometries of the plates, screws and the external and internal contours of the intact artificial right distal radius were reconstructed using Geomagic Spark (3D Systems, USA) and GOM Inspect (GOM mbH, Germany) software packages [23–25]. To simplify the models and reduce the calculation time, the screws were modelled without threads. The models of radius, plates and screws were imported and assembled within the finite element software Abaqus 6.10-1 (Dassault Systèmes, France). Each model was 85 mm long and fixed in all directions at the proximal end.

In all computational models, contact interactions using surface-to-surface and finite sliding formulation were defined between the plate and bone and between the osteotomy interfaces with a coefficient of friction of 0.3 [26]. Tied constraints were applied between the screws and plates and between the screws and the bone.

The plate constructs were meshed using 10 node quadratic tetrahedral elements. The number of elements in the models ranged from 405327 to 561167 depending on the type of plate and the number of screws (Figure 2). The element size was chosen based on a mesh convergence analysis of displacements using a model of the intact distal radius.

All material properties were defined as homogeneous, isotropic and linear. The plates and screws material was titanium alloy with an elastic modulus of 110 GPa. The moduli of elasticity used for the cortical and cancellous bone were 17 GPa and 1.3 GPa, respectively [26]. The Poisson's ratio for all materials was set to be 0.3 [26].

Non-linear computational simulations were performed for axial compression, and volar and dorsal bending. To avoid the appearance of plastic deformations, the models were loaded with 50 N. The force was chosen based on previous biomechanical studies [26]. This force was

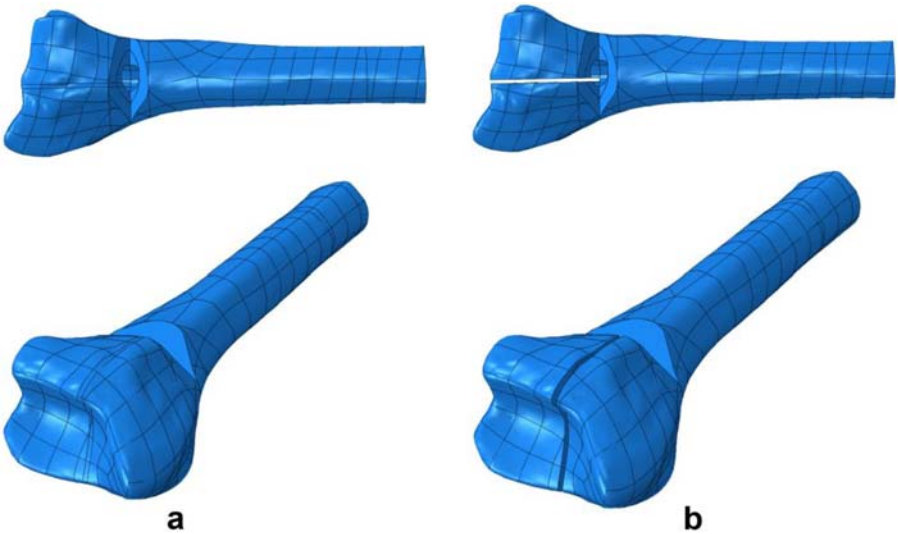

Fig. 1. Radial osteotomies: a) two-part (AO 23-A3.2), and b) three-part (AO 23-C2.1).